Available online at www.sciencedirect.com
SCIENCE DIRECT
Journal of Photochemistry and Photobiology A: Chemistry 179 (2006) 289–297
Journal of Photochemistry and Photobiology A:Chemistry
www.elsevier.com/locate/jphotochem

On the parallel formation of long-lived excited states of dipyridil[3,2-a:2′3′-c]phenazine, dppz A contrast between the electrochemically and photochemically induced reduction of dppz

G.T. Ruiz [a], M.P. Juliarena [b], R.O. Lezna [a], M.R. Feliz [b,*], G. Ferraudi [c,*]

[a] *INIFTA-CONICET, Universidad Nacional de La Plata, C. C. 16, Suc. 4, 1900 La Plata, Argentina*
[b] *INIFTA-CICBA, Universidad Nacional de La Plata, C. C. 16, Suc. 4, 1900 La Plata, Argentina*
[c] *Radiation Laboratory, Notre Dame, IN 46556-0579, USA*

Received 10 January 2005; received in revised form 31 May 2005; accepted 28 July 2005
Available online 3 October 2005

Abstract

The photophysical and photochemical properties of dipyridil[3,2-a:2′3′-c]phenazine, dppz, were investigated in homogeneous solution by time-resolved and steady-state photochemical techniques. Irradiation of dppz in CH_3OH, CH_3CN or CH_2Cl_2 induced short-lived fluorescence with a lifetime, $\tau \leq 20$ ns. Different emission quantum yields were determined when dppz was irradiated at 350 nm, $\phi_{LUM} \leq 2.5 \times 10^{-4}$, and when it was irradiated at ∼400 nm, $3.2 \times 10^{-3} \leq \phi_{LUM} \leq 2 \times 10^{-2}$. Reactions of the luminescent excited states with electron donors, TEOA or TEA, and incapacity for an inefficient H atom abstraction from 2-propanol suggested that they were ππ* excited states. Long-lived transient absorption spectra with lifetimes in the microsecond time domain were associated with adducts of the ground and excited states. The dppz radical, product of the excited state electron transfer reactions, and the product of the reduction of dppz by pulse radiolytically generated e^-_{sol} have the same UV–vis spectrum. Their spectrum differs, however, with the spectrum of the radicals from the electrochemically reduced dppz. The photophysical and photochemical results are attributed to low-lying ππ* excited states of dppz.

Keywords: Dppz; UV–vis spectrum; Photochemical techniques

1. Introduction

The photochemistry and photophysics of transition metal coordination complexes with the ligand dipyridil[3,2-a:2′3′-c]phenazine, dppz, has recently received considerable attention [1–5].

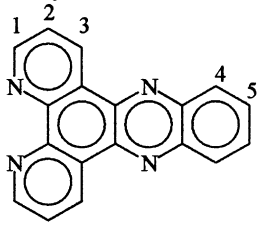

dppz with proton numbering for ^{1}HNMR

Some of the interest in this compound has been motivated by the intercalation of the dppz and its complexes in DNA and the differences between the photophysical and photochemical properties of free and intercalated dppz [1–6]. Metal to ligand charge transfer excited states are the excited states of the lowest energy in complexes where the electrochemical potentials of M(III)/M(II) couples, e.g., M = Ru, Os, or M(II)/M(I)couples, e.g., M = Re, are not very positive [7–14]. Also long-lived triplet excited states centered in the dppz ligand have been observed when the complexes are irradiated in absorption bands of the optical metal to ligand charge transfer transitions or in higher energy bands assigned to π–π* electronic transitions centered in the dppz [3,5].

In the electrochemical reduction of the coordinated dppz, the added electron can be localized in different sectors of the ligand [15,16]. These sectors have been theoretically identified as an antibonding orbital, b_1(phz), placed in the phenazine region and

* Corresponding authors.
E-mail addresses: mfeliz@inifta.unlp.edu.ar (M.R. Feliz), ferraudi.1@nd.edu (G. Ferraudi).

1010-6030/$ – see front matter © 2005 Elsevier B.V. All rights reserved.
doi:10.1016/j.jphotochem.2005.07.024

two orbitals, $b_1(\Psi)$ and $a_2(\chi)$, localized in the bipyridinic region of the ligand. The former orbital is generically described as "the redox orbital" while the latter orbitals are denominated "optical orbitals". In this work we have investigated the photophysical and photochemical properties of the dppz in different solvents by steady-state and time-resolved techniques.

2. Experimental

The experiments described herein were conducted with solutions kept at room temperature. Specific experimental procedures are described next.

2.1. Flash photochemical procedures

Absorbance changes, ΔA, occurring on a time scale longer than 10 ns were investigated with a flash photolysis apparatus described elsewhere [9–11]. In these experiments, 10 ns flashes of 351 nm light were generated with a Lambda Physik SLL-200 excimer laser. The energy of the laser flash was attenuated to values equal to or less than 20 mJ/pulse by absorbing some of the laser light in a filter solution of $Ni(ClO_4)_2$ having the desired optical transmittance, $T = I_t/I_0$ where I_0 and I_t are, respectively the intensities of the light arriving to and transmitted from the filter solution. The transmittance, $T = 10^{-A}$, was routinely calculated by using the spectrophotometrically measured absorbance, A, of the filter solution. A right angle configuration was used for the pump and the probe beams. Concentrations of the dppz were adjusted to provide homogeneous concentrations of photogenerated intermediates over the optical path, $l = 1$ cm, of the probe beam. To satisfy this optical condition, solutions were made with an absorbance equal to or less than 0.8 over the 0.2 cm optical path of the pump.

A CPA-2010 1 kHz Amplified Ti:Sapphire Laser System from Clark MXR and software from Ultrafast Systems were used for the observation of transient absorption spectra and the study of reaction kinetics in an fs to 1.6 ps time domain. The flash photolysis apparatus provides 775, 387 or 258 nm laser pulses for excitation with a pulse width of 150 fs. Data points can be collected at intervals equal to or longer than 10 fs. A slow but constant flow of the solutions through a 2 mm cuvette was maintained during the photochemical experiments.

Time-resolved fluorescence experiments were carried out with a PTI flash fluorescence instrument [9]. The excitation light was provided by a N_2 laser ($\lambda_{em} = 337$ nm, ca. 2 mJ/pulse and 200 ps bandwidth at half height). All the solutions used in the photochemical work were deaerated for 30 min with streams of ultrahigh-purity N_2 before and during the irradiations.

2.2. Steady-state irradiations

The luminescence of the compounds was investigated in a spectrofluorometer, Perkin-Elmer LS 50B, by procedures reported elsewhere [9,17]. The spectra were corrected for differences in instrumental response and light scattering. Solutions were deaerated with ultrahigh-purity N_2 in a gas-tight apparatus before recording the spectra.

Eq. (1) was used for the calculation of the quantum yield of emission, ϕ_{LUM}, by using solutions of a reference compound with a known quantum yield of emission, $\phi(\text{ref})_{LUM}$

$$\phi(\text{dppz})_{LUM} = \frac{I_{dppz}}{I_{ref}} \frac{A_{ref}}{A_{dppz}} \left(\frac{n_{dppz}}{n_{ref}} \right)^2 \phi(\text{ref})_{LUM}. \quad (1)$$

In Eq. (1), n_{dppz} and n_{ref} are the refractive indexes of the optically diluted solutions of the dppz and reference compounds, i.e., solutions with A_{ref} and $A_{dppz} < 0.1$. A solution of Rhodamine B in ethanol was used as a reference with $\phi(\text{ref})_{LUM} = 0.69$. The areas under the emission spectra of dppz and Rhodamine B were used as a relative measure of the respective intensities of the luminescence, I_{dppz} and I_{ref} [18].

Steady-state irradiations of dppz deaerated solutions were carried out with light from a 350 nm Rayonet lamp. The solutions for these experiments were placed in dual reaction cell with 1 and 0.2 cm optical paths. The cell was described elsewhere in the literature [20]. Concentrations of dppz, $[\text{dppz}] \geq 1.0 \times 10^{-4}$ M, were used in the side with 1 cm optical path in order to absorb all the incident light during the photolysis. The optical changes induced by the irradiation were investigated with the solution displaced to the chamber with a 0.2 cm optical path. Light intensities, $1 \times 10^{-3} \geq I_0 \geq 1 \times 10^{-4}$ Einstein $dm^{-3}\,min^{-1}$, were measured with Parker's actinometer [19].

2.3. Electrochemical measurements

A potentiostat PAR Model 173 with an interface module 276A and a Model 175 Universal Programmer were used for the dc and ac voltammetries [21–24]. Acetonitrile, Merck 'SeccoSolv', was dried further over activated alumina for several days. The procedure was found to be suitable for electrochemistry in the 1.5 to +0.6 V potential range. Bu_4NPF_6 was dried at 110 °C for at least 24 h. Platinum discs, polished to a mirror finish, were used as working electrodes. Potentials were measured against an $Ag/AgCl/KCl_{sat}$ electrode and are quoted with respect to the Fc/Fc^+ couple. Oxygen was removed by bubbling purified N_2 for at least 30 min prior to each experiment. Spectroelectrochemical measurements were made by modulating the electrode potential at 11 Hz around the potential of the appropriate CV wave. Reflected light with the spectroscopic information was demodulated with a lock-in amplifier. Diffraction orders higher than unity were eliminated with optical filters. The spectrum was calculated with the relationship, $\Delta R/R \equiv -\Delta A$, where R is the reflectance at the observation wavelength, λ_{ob}, and A the absorbance. Measurements in the entire spectral region were made by maintaining the value of R constant. To fulfill this condition, a feedback circuit maintained a constant current through the photomultiplier.

2.4. Pulse-radiolytic procedures

Pulse radiolysis experiments were carried out with a model TB-8/16-1S electron linear accelerator. The instrument and computerized data collection for time-resolved UV–vis spectroscopy and reaction kinetics have been described elsewhere in the

literature [25,26]. Thiocyanate dosimetry was carried out at the beginning of each experimental session. The details of the dosimetry have been reported elsewhere [25–30]. The procedure is based on the concentration of $(SCN)_2^-$ radicals generated by the electron pulse in a N_2O saturated 10^{-2} M SCN^- solution. In the procedure, the calculations were made with $G = 6.13$ and an extinction coefficient, $\varepsilon = 7.58 \times 10^3\ M^{-1}\ cm^{-1}$ at 472 nm, for the $(SCN)_2^-$ radicals [25,27]. In general, the experiments were carried out with doses that in N_2 saturated aqueous solutions resulted in $(2.0 \pm 0.1) \times 10^{-6}$ to $(6.0 \pm 0.3) \times 10^{-6}$ M concentrations of e^-_{sol}. In these experiments, solutions were prepared by the procedure indicated above for the photochemical experiments. The liquids were deaerated with streams of the O_2-free gas, N_2 or N_2O, that was required for the experiment. In order to radiolyze a fresh sample with each pulse, an appropriate flow of the solution through the reaction cell was maintained during the experiment. Other conditions used for the time-resolved spectroscopy of the reaction intermediates or in the investigation of the reaction kinetics are given in Section 3. Radiolyses with ionizing radiation of CH_3OH and CH_3OH/H_2O mixtures have been reported elsewhere in the literature [27–29]. These studies have shown that pulse radiolysis can be used as a convenient source of e^-_{sol} and $CH_2OH^\bullet$ radicals, Scheme 1.

Since e^-_{sol} and $CH_2OH^\bullet$ have large reduction potentials, i.e., −2.8 V versus NHE for e^-_{sol} and −0.92 V versus NHE for $CH_2OHOH^\bullet$, they have been used for the reduction of coordination complexes and for the study of electron transfer reactions. The yield of e^-_{sol} in CH_3OH ($G \approx 1.1$) [27], is about one third of the G-value in the radiolysis of H_2O ($G \approx 2.8$) [29]. In solutions where e^-_{sol} was scavenged with N_2O, the $CH_2OH^\bullet$ radical appears to be the predominant product (yield > 90%) of the reaction between CH_3OH and $O^{\bullet -}$.

2.5. Materials

The dppz and 1,10-phenanthroline-5,6,-dione were prepared by a literature procedure [31,32]. The melting point, the UV–vis spectrum and the half-wave potential of the dppz/dppz$^-$ couple, $E_{1/2} = -1.19$ V versus Ag/AgCl/KCl_{sat}, were all in good agreement with those communicated in literature reports [33].

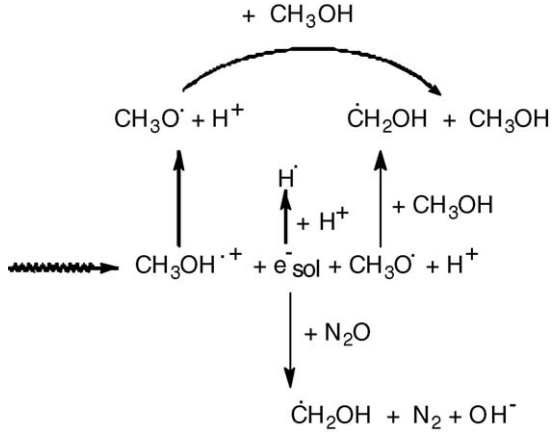

Scheme 1.

Furthermore, the ^1H NMR spectra of the samples used for the photochemical work indicated that they were free of major impurities which could have affected the experimental results. The 250 MHz dppz's ^1H NMR in CD_3CN, exhibited the following resonances: H (standard solvent signal) 9.597 (H3, dd), 9.203 (H1, dd), 8.366 (H4, dd), 8.004 (H5, dd), and 7.867 (H2, dd) with the proton numbering given in Section 1. To verify that the results of the photophysical experiments were not affected by impurities that remained undetected with the previous analyses, samples of the dppz, already purified by recrystallization according to the literature procedure, was sublimated under vacuum, i.e., ∼0.2 g sublimated at ∼443 K under a pressure of ∼0.027 Torr. The pale yellow material and the material purified only by recrystallization showed the same UV–vis spectrum and insignificant differences in their photophysical properties.

Other materials were reagent grade and used without further purification.

3. Results

3.1. UV–vis absorption spectroscopy

The UV–vis spectrum of dppz agreed with the literature spectrum [31–33]. It obeys the Beer's law in protic and aprotic solvents when the concentration of dppz is equal to or less than 3×10^{-4} M. No oligomers are formed under these experimental conditions. Only small differences were observed between the UV–vis spectrum of dppz in various solvents, i.e., CH_2Cl_2, CH_3CN or CH_3OH. Such small changes are expected for the medium effects on the $n\pi^*$ and $\pi\pi^*$ electronic transitions and they cannot be attributed to the displacement of a chemical equilibrium between species. About 13 spectroscopic features can be discerned in the spectrum between 200 and 400 nm. Vibronic structure is seen between 340 and 380 nm in the first intense band.

3.2. Luminescence

The emission spectrum exhibited a dependence on the concentration of dppz, Fig. 1a. Since the dependence of the absorbance on dppz concentration obeys the Beer's law, the effect of the dppz concentration on the luminescence was adjudicated to an excited state process. That the process was a reaction between the excited state and the ground state of dppz was established in a time-resolved investigation of the luminescence. These experimental observations are described elsewhere in this work. The dppz's emission spectrum also exhibited a dependence on excitation wavelength, λ_{exc}, Fig. 1b. To investigate the dependence of the emission on λ_{exc}, 10^{-5} to 10^{-4} M solutions of dppz, i.e., concentrations that make the absorbance ∼0.1 in a 1 cm optical path at λ_{exc}, were irradiated at several wavelengths, i.e., $\lambda_{exc} = 350$, 380, 400 and 420 nm.

In the absorption spectrum of dppz, the wavelengths 350 and 380 nm correspond to a shoulder in a complex band while the wavelengths 400 and 420 nm correspond to the higher energy side of the same band. A maxima at ∼466 nm and a shoulder at

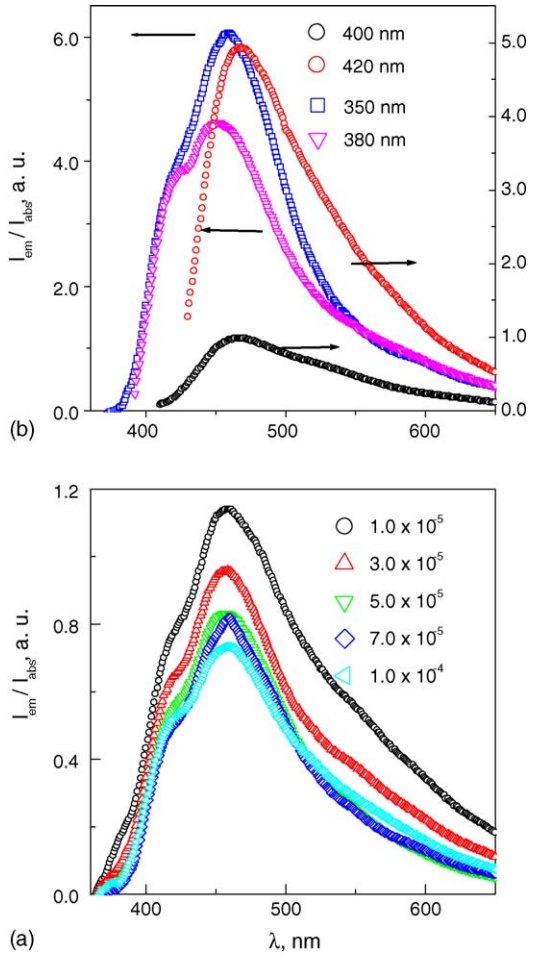

Fig. 1. Emission spectra of 1.1×10^{-4} M dppz in CH_2Cl_2. (a) Dependence of the emission spectrum on the dppz concentration. (b) Dependence of the spectrum on excitation wavelength. The wavelength of the excitation, λ_{exc}, is indicated in the figure. The spectra in (a) and (b) are normalized to the intensity of light absorbed by dppz at the wavelength of excitation.

~538 nm can be seen in the emission spectrum of dppz when $\lambda_{exc} = 400$ or 420 nm. By contrast, the maximum is at ~457 nm in the emission spectrum when $\lambda_{exc} = 350$ or 380 nm. The two bands have a considerable overlap when the emission of dppz was investigated in CH_2Cl_2. Two different sources of the luminescence account for these experimental observations and for the dependence of the excitation spectrum on the monitoring wavelength, λ_{ob}. Large differences were observed between the excitation spectra recorded, respectively, with $\lambda_{ob} = 450$ and 510 nm, i.e., near the maxima of the two bands in the emission spectrum, Fig. 2. In relative terms, the emission at 510 nm is more intense when dppz is irradiated in the shoulder at 420 nm than at $\lambda_{exc} \leq 380$ nm. The order of intensities is reversed when the luminescence is monitored at 450 nm. Luminescence quantum yields for the 350 or 400 nm irradiation of dppz in different media are presented in Table 1. They reveal that irradiation at 400 nm induces a more intense emission than the irradiation at 350 nm.The effect of proximate $\pi\pi^*$ and $n\pi^*$ excited states has been discussed in the literature in connection with the photophysics of the azines [34–37]. On this basis, when dppz is irradiated at 400 nm the solvent dependence of the emission

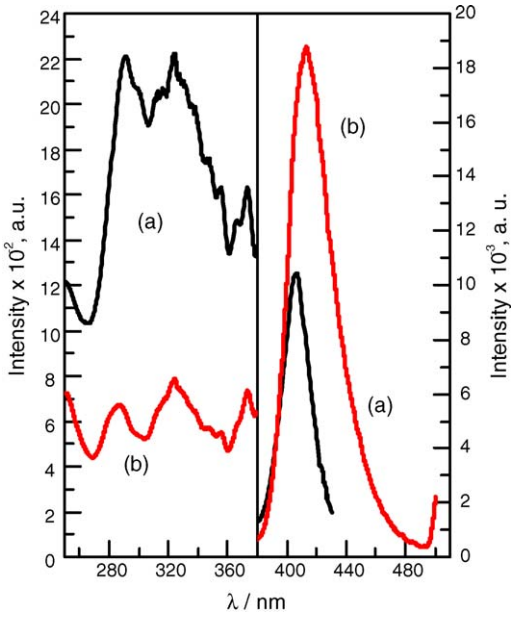

Fig. 2. Excitation spectrum of 10^{-4} M dppz in CH_2Cl_2. The emission was monitored at $\lambda_{ob} = 450$ nm (a) and $\lambda_{ob} = 510$ nm (b).

quantum yield can be associated with a luminescent lowest lying $\pi\pi^*$ excited state which has a neighboring $n\pi^*$ excited state positioned at a higher energy. The values of the emission quantum yield measured when dppz was irradiated at $\lambda_{exc} = 350$ nm show the reverse order of the quantum yields obtained when the irradiation was carried out at $\lambda_{exc} = 400$ nm. This reverse order suggests a more efficient deactivation of the emissive $\pi\pi^*$ excited state by the $n\pi^*$ excited state.

Flash irradiation, $\lambda_{exc} = 337$ nm, of 9.0×10^{-5} M dppz in a variety of solvents, i.e., CH_2Cl_2, CH_3CN or CH_3OH, induced a short-lived luminescence with a biphasic decay. One component, $\tau \leq 2.0$ ns, was convoluted with the laser pulse. The other component was fitted to an exponential with a lifetime, $17.0 \leq \tau \leq 20.0$ ns, that was independent of the monitoring wavelength and did not change when solutions of dppz were acidified with HCH_3SO_3, Table 1. There is, however, a linear dependence of the reciprocal of the lifetime on the dppz concentration consistent with the dependence of the emission spectrum on dppz concentration. Self-quenching of the luminescence's long-lived component with a rate constant,

Table 1
Photophysical properties of dppz as a function of solvent and excitation wavelength

Solvent	τ_{LUM} (ns)[a]	ϕ_{LUM}		Acid concentration
	$\lambda_{ob} = 530$ nm	$\lambda_{exc} = 350$ nm	$\lambda_{exc} = 400$ nm	
CH_2Cl_2	18.8	2.5×10^{-4}	3.2×10^{-3}	[b]
CH_3CN	16.2	2.3×10^{-4}	1.2×10^{-2}	[b]
	18.4			10^{-4} M CH_3SO_3H
	20.0			>1 M CH_3SO_3H
CH_3OH		1.9×10^{-4}	1.8×10^{-2}	[b]

[a] Lifetimes calculated from traces recorded in the PTI flash fluorescence instrument. Solutions containing 9.0×10^{-5} M dppz were irradiated at 337 nm.
[b] No acid added.

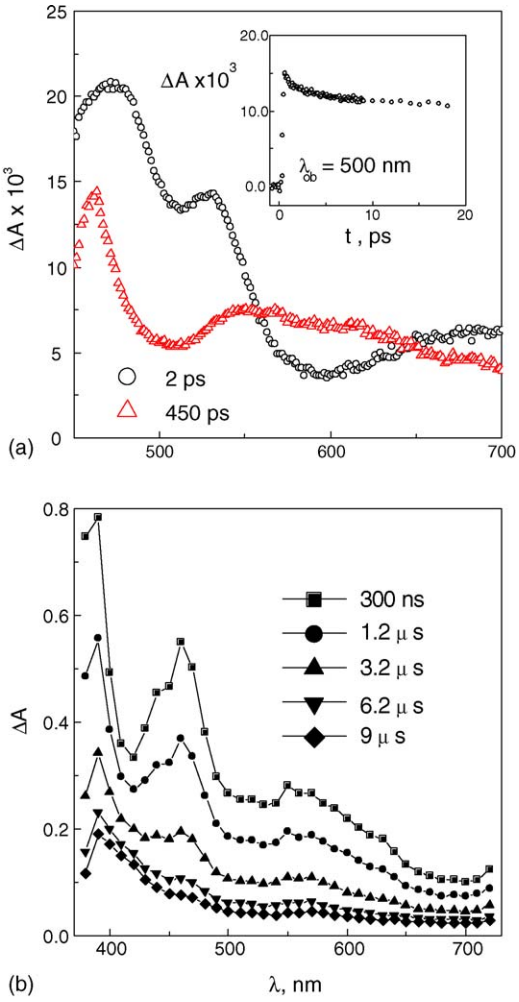

Fig. 3. Transient spectra observed in flash photolysis experiments. (a) Excited state transient spectra recorded with 2 ps and 450 ps delays from the 387 nm laser flash irradiation of 10^{-4} M dppz in CH_3CN. (b) Excited state transient spectra recorded with different delays from the 351 nm laser flash irradiation of 10^{-4} M dppz in CH_3CN.

$k_q = (4.5 \pm 1.5) \times 10^{11}\ M^{-1}\ s^{-1}$, accounts for both experimental observations. Therefore, the self-quenching processes will have an effect on the experimental observations when the concentrations of dppz are equal to or larger than 2×10^{-5} M, a concentration where 15% of the excited state is quenched by the ground state.

3.3. Time-resolved UV–vis absorption spectroscopy of transient species

As could be expected from the previously recounted experimental observations, flash irradiated solutions of dppz exhibited spectral changes in the fs to 1.6 ns time range. Traces recorded, $\lambda_{exc} = 387$ nm, in this time domain showed a decay of the prompt generated absorbance with a lifetime, $\tau \approx 7.5$ ps, Fig. 3a. Due to the time scale of the observation, the process with $\tau \approx 7.5$ ps must be assigned to intersystem crossing processes of prompt generated singlet states into longer-lived triplet states. This observation is in accordance with an earlier communication in the literature [38]. A subsequent slower decay of the absorbance with a lifetime, $\tau \geq 2$ ns, was beyond the time domain accessible to the instrument. However, the difference spectrum recorded 300 ps after the irradiation was the same observed in at ~20 ns time domain in another instrument with a slower time response. It can be assigned to excited states giving rise to the 17–20 ns emission.

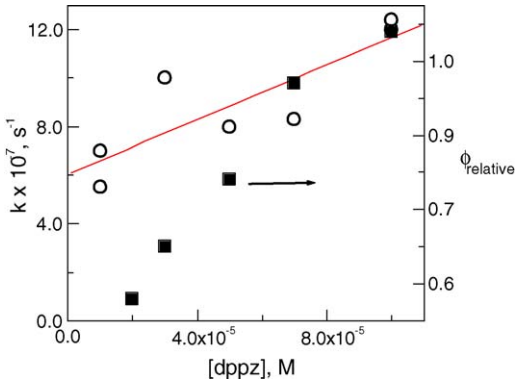

Fig. 4. Dependence on the dppz concentration of the rate constant for the decay of the transient spectrum, (◯) and left axis. The decay was observed on a time scale 300 ps < t < 100 ns. The dependence of the relative yield of product formed in this decay of the spectrum, (■), is plotted against the right axis. Yields of product were evaluated at 300 ns, i.e., more than five time the lifetime of the excited states, after the laser irradiation. In these experiments, solutions of dppz in CH_3CN were irradiated at 351 nm.

In addition to the transient spectrum with 17–20 ns lifetime, the transient spectra of longer-lived species were recorded in a 1–60 μs time domain when solutions containing 2×10^{-5} to 2×10^{-4} M dppz in CH_3CN were flash irradiated at 351 nm, Fig. 3b. The transient spectra recorded with delays equal to or longer than 10^2 ns, i.e., five times longer than the lifetime of the luminescence, exhibited maxima at 390, 460 and 550 nm and a biphasic decay. To verify that these long-lived transients were products of the reaction between the triplet states and the dppz ground state, the lifetime of the excited state and the yield of products were measured as a function of the dppz concentration, Fig. 4. A relative quantum yield of the transient species was calculated when the 460 nm absorbance change, ΔA_{460}, recorded 300 ns after the laser irradiation, was divided by the absorbed intensity of the laser light, I_{ab}/I_0, relative to the intensity of the incident laser light. This absorbed intensity was, $I_{ab}/I_0 = (1 - 10^{-A_{351}})$, where A_{351} is the absorbance of the dppz solution at 351 nm. The relative measure of the quantum yield of the transient species exhibited a linear dependence on the dppz concentration as it is expected for the reaction of an excited state with the ground state.

In accordance with the quenching of the luminescence, the products of this reaction are formed in less than a 100 ns and they disappear in 10^2 μs with a complex kinetics. The biphasic decay of the long-lived products was investigated at 460 nm as a function of the dppz concentration. In the range of dppz concentration from 2×10^{-5} to 2×10^{-4} M, the biphasic decay of the transient spectrum exhibited the kinetics expected for two consecutive reactions that are kinetically of a first order and a second order. Indeed, oscillographic traces obtained from flash

photolysis experiments with a 2×10^{-5} M dppz solution showed deviations from an exponential, $\Delta A_0 \exp(-k_T \times t)$, where ΔA_0, is the absorbance change 300 ns after the laser irradiation and $k_T = (2.5 \pm 0.3) \times 10^5\ s^{-1}$. The deviations from the exponential decay became more pronounced with an increasing concentration of dppz. When 2×10^{-4} M dppz was flash photolysis irradiated, the dependence of the reciprocal of the flash induced change in the 460 nm absorbance, $1/\Delta A_{460}$ on time was almost linear, i.e., it approached close to a rate law with a second order on reactant concentration. The ratio of the rate constant to the extinction coefficient, $2k_3/\Delta\varepsilon = 1.0 \times 10^6\ cm\ s^{-1}$, was calculated from the plot of $1/\Delta A_{460}$ versus t. Values of $2k_3/\Delta\varepsilon$ and k_T were also calculated from a nonlinear squares fitting of the oscillographic traces by Eq. (2).

$$\frac{\Delta A_\lambda(t)}{\Delta A_\lambda(0)} = \exp(-k_T t) + \frac{\Delta\varepsilon}{\Delta\varepsilon^*} k_2 k_T t^2 + \frac{\Delta\varepsilon}{\Delta\varepsilon^*} \times \left(-\frac{2}{3} \frac{\Delta A_\lambda(0)}{\Delta\varepsilon^*} k_2^2 k_3 + \frac{1}{6} k_2 k_T^2 \right) t^3. \quad (2)$$

Eq. (3) is an analytical expression of the absorbance change when a photogenerated species R^*, with an extinction coefficient ε^*, forms transient products, P_1 and P_2, whose extinction coefficients are, respectively, ε_1 and ε_2, Eqs. (3)–(5).

$$R \xrightarrow{h\nu,\phi} R^* \xrightarrow{k_1} R \quad (3)$$

$$R^* \xrightarrow{k_2} P_1 + P_2 \quad (4)$$

$$P_1 + P_2 \xrightarrow{2k_3} R \quad (5)$$

In Eq. (2), $\Delta A_\lambda(0)$ and $\Delta A_\lambda(t)$ are the photoinduced absorbance changes at the observation wavelength λ. They have been, measured, respectively at the beginning of the reaction and at an instant t. Other parameters in Eq. (2) are the relative extinction coefficients, $\Delta\varepsilon^* = \varepsilon^* - \varepsilon_A$ and $\Delta\varepsilon = \varepsilon_1 + \varepsilon_2 - 2\varepsilon_A$ where ε_A is the extinction coefficient of A and $k_T = k_1 + k_2$. The values of $2k_3/\Delta\varepsilon$ and k_T, calculated with Eq. (2), $2k_3/\Delta\varepsilon = 2 \times 10^6\ cm\ s^{-1}$ at 460 nm and $k_T = 2.1 \times 10^5\ s^{-1}$, agreed with those reported above for the limiting kinetics.

Similar transient spectra were recorded in the 351 nm photolysis of 2.5×10^{-5} M dppz in CH_2Cl_2. A displacement of the maximum ~10 nm toward the red and a marginally slower decay kinetics were the differences between the transients generated in CH_2Cl_2 and CH_3CN.

3.4. Scavenging of transient species

One characteristic reaction of $n\pi^*$ excited states is the abstraction of H atoms from primary and secondary alcohols. However, the spectra and decay kinetics of the transients observed when 1.2×10^{-4} M dppz and 9.3×10^{-1} M 2-propanol in CH_3CN were irradiated at 351 nm were the same of those transients generated in the absence of 2-propanol. It must be concluded that the abstraction of hydrogen from 2-propanol by $n\pi^*$ excited states of dppz is an inefficient process. The continuous dppz photolysis has also shown that 2-propanol

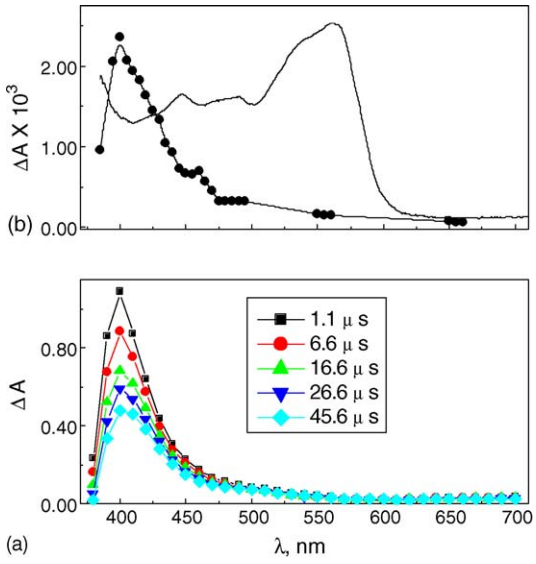

Fig. 5. Transient spectra (a) recorded with different delays from the 351 nm laser flash irradiation of 1.2×10^{-4} M dppz and 0.93 M TEOA in CH_3CN. In (b) the spectrum recorded when 1.0×10^{-4} M dppz in CH_3OH is reduced by e^-_{sol}, (●), and the spectrum, (–), of the $dppz^{\bullet-}$ radical generated when 3.0×10^{-4} M dppz in CH_3CN is reduced over a Pt working electrode modulated between −1500 and −600 mV at 11 Hz. A Ag/AgCl electrode was used as a reference electrode. The angle of incidence of the probe is 45° and the support electrolyte is 0.1 M Bu_4NPF_6.

undergoes some inefficient redox processes with the excited states. A similarly inefficient reaction between electronically excited phenazine and 2-propanol has been communicated elsewhere in the literature [39].

In contrast to the poor reactivity with 2-propanol, the transient with $\lambda_{max} = 460, 550$ nm readily reacted with 9.3×10^{-1} M TEOA. The decay of the reaction with 2-propoanol is kinetically of a second order on the product's concentration, i.e., plots of $1/\Delta A$ versus t were linear. A ratio of the rate constant to the extinction coefficient, $2.5 \times 10^4\ cm\ s^{-1}$, was calculated from the slope of $1/\Delta A_{400}$ versus t, where ΔA_{400} is the absorbance change at 400 nm. The expected product of the reaction is the protonated radical $dppzH^{\bullet}$. Protonation of the radical is proposed in accordance with the strong base character of the pyridinyl radicals [40,41]. However, pronounced differences were seen between the spectrum of the transient product and the spectrum of the electrochemically generated $dppz^{\bullet-}$ radical, Fig. 5a and b. In Fig. 5b, the spectrum of the $dppzH^{\bullet}$ radical obtained by the spectroelectrochemical technique is in excellent agreement with the literature spectrum [42]. To confirm the nature of the species observed in the already described flash photolysis experiments, dppz in methanol was reduced with pulse-radiolytically generated e^-_{sol}. This product and the reaction product generated in the flash irradiation of dppz in the presence of TEOA exhibited the same spectrum, Fig. 5b. The redox potentials of the $CH_2O/CH_2OH^{\bullet}$ and $dppz/dppz^{\bullet-}$ show that the reduction of the dppz by $CH_2OH^{\bullet}$ has a Gibs free energy, $G^0 > 0$. In accordance with the endoergonicity of the reaction, no transient spectrum indicative of a reaction between $CH_2OH^{\bullet}$ and dppz was observed in pulse radiolysis experiments with N_2O-saturated solutions of dppz. The spectroscopic differences

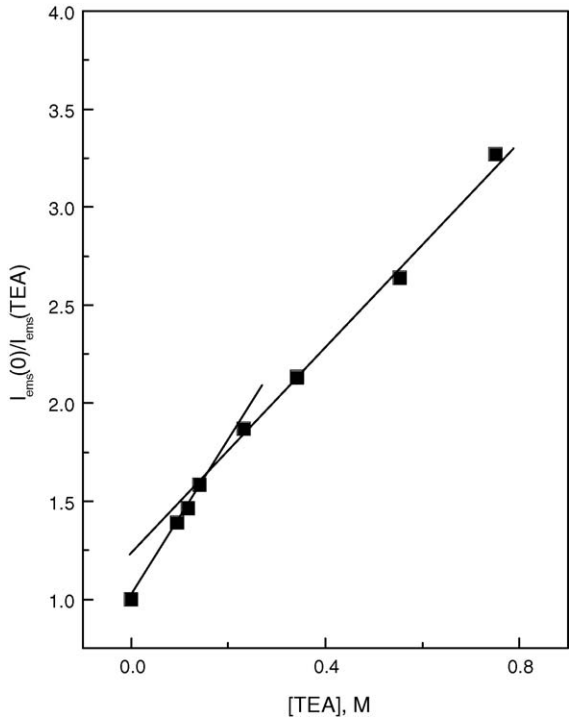

Fig. 6. Stern–Volmer plot for the quenching of the dppz emission by TEA. The solutions, 2×10^{-5} M dppz and a given concentration of TEA in CH_3CN were irradiated at $\lambda_{exc} = 350$ nm.

between the electrochemically and photochemically generated radicals are accounted for the formation of adducts, $(dppz)_2H^{\bullet}$, when the concentration of dppz is equal to or larger than 10^{-3} M. Indeed, the spectrum of the pulse-radiolytically generated radical approaches the spectrum of the electrochemically generated radical as the concentration of dppz is increased in accordance to Eq. (6) (G. Ruiz, G. Ferraudi, in preparation).

$$dppz \xrightarrow{e^- + H^+} dppzH^{\bullet} \underset{-dppz}{\overset{+dppz}{\rightleftarrows}} (dppz)_2H^{\bullet} \quad (6)$$

3.5. Quenching of the luminescence

In steady-state irradiations of 2×10^{-5} M dppz in CH_3CN, the quenching of the luminescence with 0.8 to 10^{-2} M 2,2′,2″nitrilotriethane, TEA, in CH_3CN also supported the fact that two different excited states were the sources of the dppz luminescence. The data in a Stern–Volmer plot drawn for the quenching of the dppz luminescence when $\lambda_{exc} = 350$ nm had to be fitted to two lines with slopes $K_{SV,1} = 4.3\ M^{-1}$ and $K_{SV,2} = 3\ M^{-1}$, Fig. 6. Since no changes were observed in the UV–vis spectrum of dppz in the mentioned range of TEA concentration, formation of a ground state adduct between TEA and dppz cannot be responsible for the decreasing intensity of the dppz luminescence with TEA concentration. Also, the low concentration of dppz prevented the formation of scavengeable products of the reaction between excited and ground state dppz. The two quenching regimes must be assigned to reactions of TEA with two different excited states.

The lifetime of the luminescence and time-resolved absorption spectroscopy, $\tau = 16.2$ ns, induced when dppz is irradiated in CH_3CN, Table 1, can be combined with $K_{SV,1} = 4.3\ M^{-1}$ to give a quenching rate constant for the reaction with TEA, $k_q = K_{SV,1}/\tau = 2.6 \times 10^8\ M^{-1}\ s^{-1}$. A reason for the smaller value of the Stern–Volmer constant, $K_{SV,2} = 3\ M^{-1}$, for the second component of the Stern–Volmer plot reason is that the quenched excited state undergoes a relaxation to the ground state with a lifetime $\tau = 7.5$ ps. Because the lifetime is shorter than the time response of our flash fluorescence instrument, the emission from this excited state was convoluted with the laser pulse in our flash-fluorescence experiments. It was detected, however, in our time-resolved spectroscopy, i.e., experiments in a time domain of fs to ns. This excited state must be quenched, therefore, with a diffusion controlled rate, i.e., $k_q = K_{SV,2}/\tau = 4.0 \times 10^{11}\ M^{-1}\ s^{-1}$.

4. Discussion

A comparison between the UV–vis absorption spectra of the dppz and the related compound, dipyridil[3,4-b:2′,3′-c]phenazine, reveal some of their common spectral features. In the spectrum of dipyridil[3,4-b:2′,3′-c]phenazine, theoretical calculations predicted a low intensity band at ∼470 nm corresponding to the $^1(n\pi^*) \leftarrow S_0$ transition [43]. This optical transition appears, however, at a shorter wavelength, i.e., 438.6 nm, in the spectrum of dipyridil[3,4-b:2′,3′-c]phenazine. The first intense band in the spectrum of dipyridil[3,4-b:2′,3′-c]phenazine has been assigned to a $^1(\pi\pi^*) \leftarrow S_0$ transition and correlates with the first intense and structured band in the spectrum of dppz.

The features of the emission and excitation spectra of dppz, Figs. 1 and 2, must be rationalized on the basis of two isolated sources of the luminescence. Species in a thermal equilibrium with dppz, i.e., ground state adducts and/or high concentrations of impurities functioning as different sources of the luminescence can be discounted. They were undetected in the ^1H NMR and UV–vis spectra and no significant differences were observed in the spectroscopy and photophysics of dppz samples subjected to different purification procedures. The sources have, therefore, been ascribed to two different manifolds of excited states. In addition, products formed of the reaction between electronically excited dppz and ground state dppz have much longer lifetimes than the lifetimes of the luminescence. If they are electronically excited adducts, i.e., excimers, their luminescence must have a small quantum yield that prevented their observation in our experiments.

The irradiation of dppz at $\lambda_{exc} = 350$ nm induces luminescence with 10 to 100 times smaller quantum yields than the irradiation at 400 nm, Table 1. Moreover, the solvent dependence of the luminescence quantum yield when $\lambda_{exc} = 350$ nm is the one expected when a fluorescent $^1\pi\pi^*$ is partially converted to a $n\pi^*$ excited state or the $n\pi^*$ excited state is itself the source of the phosphorescence [34–37]. The low efficiency of the reaction between the excited states of dppz with 2-propanol does not support, however, the latter proposition. By contrast to the irradiation of dppz at 350 nm, the quantum yield of the luminescence induced when dppz is irradiated at 400 nm has the

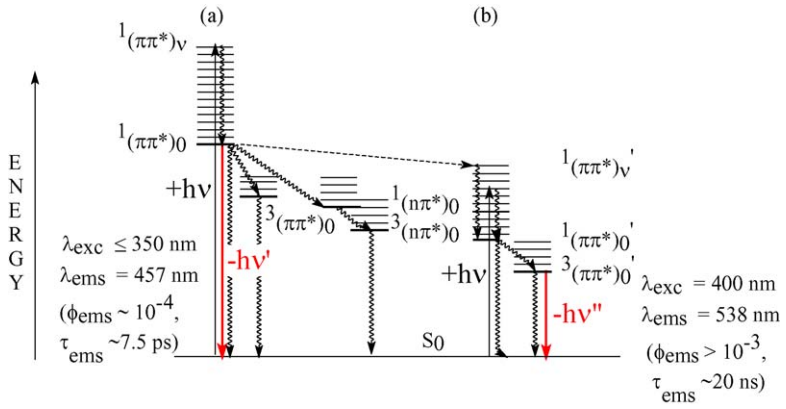

Fig. 7. Jablonski diagram for the radiationless and radiative relaxation of excited states populated when dppz is irradiated, respectively, at λ_{exc} ~400 nm and λ_{exc} ~350 nm. It shows upper $^1(\pi\pi^*)$ excited states being depopulated by a $^3(n\pi^*)$. The reaction of the long-lived escited state with the ground state of dppz has not been included in the diagram.

dependence on solvent polarity usually associated with a fluorescent $^1\pi\pi^*$. These arguments are graphically represented in the Jablonski diagram in Fig. 7. In Fig. 7a the diagram shows a $^1(n\pi^*)_0$ deactivating the $^1(\pi\pi^*)_\nu$ excited state and undergoing a non-radiative decay to the ground state. In this manifold of excited states, the fluorescence quantum yield is small, ϕ_{LUM} ~10^{-4}, because the $^1(\pi\pi^*)_\nu$ populated with 350 nm photons is partially converted to the $^3(n\pi^*)_0$ with or without participation of the $^1(n\pi^*)_0$. In the other manifold, Fig. 7b, the population of the $^1(\pi\pi^*)'_\nu$ with 400 nm photons induces luminescence with a larger quantum yield, ϕ_{LUM} ~10^{-2}. It is tempting to ascribe the origins of the $(\pi\pi^*)'_\nu$ and $(\pi\pi^*)_\nu$ manifolds to different π^* orbitals of the dppz as is the case in the photphysics of transition metal complexes of dppz.

Since $^3(\pi\pi^*)'_\nu$ and $^1(\pi\pi^*)_0$ disappear with the lifetime of the dppz's luminescence, i.e., $\tau \leq$20 ns, they cannot be related to the long-lived transient UV–vis spectra shown in Fig. 3b.The dependence of the yield on dppz concentration and the autoquenching of the luminescence indicate that the spectra in Fig. 3b must be associated with products of the reaction between the electronically excited dppz and ground state dppz. In addition, the spectra at times t >1 μs has a strong resemblance with the spectrum of the $dppz^{\bullet-}$ radical. A mechanism, Eqs. (4)–(6), consistent with these observations and the kinetics of spectrum decay may involve the formation of an excimer, Eqs. (7)–(12).

$$\mathrm{dppz} \xrightarrow{h\nu,\phi} \mathrm{dppz}* \quad (7)$$

$$\mathrm{dppz}* \rightarrow \mathrm{dppz} \quad (8)$$

$$\mathrm{dppz}* \rightarrow \mathrm{dppz} + h\nu' \quad (9)$$

$$\mathrm{dppz} * \xrightarrow{\mathrm{dppz}} (\mathrm{dppz})_2^* \quad (10)$$

$$(\mathrm{dppz})_2^* \xrightarrow{k_{2'}+H^+} \mathrm{dppzH}^\bullet + \mathrm{O}^{\bullet+} \quad (11)$$

$$\mathrm{dppzH}^\bullet + \mathrm{O}^{\bullet+} \xrightarrow{2k_{3'}-H^+} \mathrm{dppz} + \mathrm{O} \quad (12)$$

Eqs. (8)–(10) occur on the time scale of the luminescence with an overall rate constant $k_T \approx 2 \times 10^5\ s^{-1}$, Eq. (2), and $O^{\bullet+}$ in Eqs. (11) and (12) can be $dppz^{\bullet+}$ and/or a radical from the solvent. The rate constants k_2 and $2k_3$, Eqs. (11) and (12), are similar to those defined in Eqs. (4) and (5). In order to account for the experimental observations, the $(dppz)_2$* spectrum must be first observed at ~300 ns as in Fig. 3b and the spectra at a time longer than t >1 μs must be a combination of the protonated dipyridil[3,2-a:2′3′-c]phenazininyl and cation radical species spectra.

Electronically excited dppz, dppz*, reacts inefficiently with 2-propanol and efficiently with TEA and TEOA. Although, these processes must occur via electron transfer or H-abstraction reactions, the former mechanism is in better agreement with the assignment of the transient spectra in Fig. 3a to $^1(\pi\pi^*)_1$ and $^3(\pi\pi^*)'_1$ excited states. The $n\pi^*$ excited states shown in Fig. 7 are expected to be too short-lived and/or devoid of the energy necessary to drive an H-abstraction reaction from secondary or primary alcohols. A similar photobehavior of the lowest lying $n\pi^*$ excited states in azines and phthalocyanines has been communicated in literature reports [34–37,44]. In addition to the lack of a proper electronic distribution for an H-abstraction in the $^1(\pi\pi^*)_1$ and $^3(\pi\pi^*)'_1$ excited states, these excited states are devoid of the energy necessary for the H-abstraction. Based on the electrochemical potential, $E^0 \sim -1.0$ V versus NHE, for the dppz/$dppz^{\bullet-}$ couple and a photonic energy of ~200 kJ/mol for the 0–0 transition, the $\pi\pi^*$ excited states must have a marginal excess energy over the ~100 kJ/mole required for the H-abstraction from 2-propanol. Therefore, the H-abstraction from 2-propanol by the $\pi\pi^*$ excited states is expected to be a slow and inefficient process. The point has been shown in the flash photolysis experiments with dppz and in literature on works with phenazine [39]. The thermochemical restrictions are less stringent when the redox process involves an electron transfer between reactants. Indeed, the reduction potential of the electronically excited dppz couple dppz*/$dppz^{\bullet-}$ is E^0 ~1.0 V versus NHE, when the energy of the 0–0 transition is added to the reduction potential of the ground state couple. In accordance with the Marcus–Jortner theory, the dppz* reduction potential is large enough for outer sphere electron transfers with a small reorganization energy, i.e., one whose largest contribution is provided by the work terms. On this basis, the reaction between dppz* and 2-propanol, $E^0 \approx 0.90$ V versus NHE for the

$(CH_3)_2(C^{\bullet})OH/(CH_3)_2CHOH$ couple has a small driving force whereas TEOA, $E^0 \approx 0.82$ V versus NHE for the $TEOA^{\bullet+}$/TEOA couple, has the driving force necessary to overcome the reorganization energy.

Acknowledgments

GF acknowledges support from the Office of Basic Energy Sciences of the U.S. Department of Energy. This is contribution No. NDRL-4527 from the Notre Dame Radiation Laboratory. GR acknowledges support from Fundación Antorchas. We thank Mr. I. Robel, Dr. E. Wolcan and Dr. J. Guerrero for their assistance with various experiments.

References

[1] A. Kirsch-De Mesmaeker, J.-P. Lecomte, J.M. Kelly, Top. Curr. Chem. 177 (1996) 25–76.
[2] H.D. Stoeffler, N.B. Thornton, S.L. Temkin, K. Schanze, J. Am. Chem. Soc. 117 (1995) 7119–7128.
[3] J. Dyer, W.J. Blau, C.G. Coates, C.M. Creely, J.D. Gavey, M.W. George, D.C. Grills, P. Matousek, J.J. McGarvey, J. McMaster, A.W. Parker, M. Towrie, J.A. Weinstein, Photochem. Photobiol. Sci. 2 (2003) 542–554.
[4] V.W.-W. Yam, K.K.-W. Lo, K.-K. Cheung, R.Y.-C. Kong, J. Chem. Soc. Dalton Trans. (1997) 2067–2072.
[5] W.D. Bates, P.Y. Chen, D.M. Dattelbaum, W.E. Jones, T.J. Meyer, J. Phys. Chem. A 103 (1999) 5227–5231.
[6] T. Phillips, I. Haq, H.M. Meijer, H. Adams, I. Soutar, L. Swanson, M.J. Sykes, J.A. Thomas, Biochemistry 43 (2004) 13657–13665.
[7] K.S. Shanze, D.B. MacQueen, T.A. Perkins, L.A. Cabana, Coord. Chem. Rev. 122 (1993) 63–89.
[8] M.R. Feliz, G. Ferraudi, Inorg. Chem. 43 (2004) 1551–1557.
[9] J. Guerrero, O.E. Piro, E. Wolcan, M.R. Feliz, G. Ferraudi, S.A. Moya, Organometallics 20 (2001) 2842–2853.
[10] M.R. Feliz, G. Ferraudi, H.J. Altmiller, Phys. Chem. 96 (1992) 257–264.
[11] M.R. Feliz, G. Ferraudi, J. Phys. Chem. 96 (1992) 3059–3062.
[12] L.A. Worl, R. Duesing, P. Chen, L. Della Ciana, T.J. Meyer, J. Chem. Soc. Dalton Trans. (1991) 849–858.
[13] D.R. Striplin, G.A. Crosby, Chem. Phys. Lett. 221 (1994) 426–430.
[14] C.J. Kleverlaan, D.J. Stufkens, I.P. Clark, M.W. George, J.J. Turner, D.M. Martino, H. van Willegen, A. Vlèek Jr., J. Am. Chem. Soc. 120 (1998) 10871–10879.
[15] S. Berger, J. Friedler, R. Reihardt, W. Kaim, Inorg. Chem. 43 (2004) 1530–1538.
[16] S. Ernst, C. Vogler, A. Klein, W. Kaim, S. Záliš, Inorg. Chem. 35 (1996) 1295–1300.
[17] M.R. Feliz, F. Rodriguez Nieto, G. Ruiz, E. Wolcan, J. Photochem. Photobiol. A: Chem. 117 (1998) 185–192.
[18] J.C. Scaiano, Handbook of Photochemistry, vol. 1, CRC Press, Boca Raton, 1989.
[19] C.G. Hatchard, C.A. Parker, Proc. R. Soc. Lond. Ser. A 235 (1956) 518–536.
[20] G. Ferraudi, Inorg. Chem. 19 (1980) 438–444.
[21] R.O. Lezna, An. Asoc. Quím. Argent. 76 (1988) 25–44.
[22] R.O. Lezna, An. Asoc. Quím. Argent. 82 (1994) 293–304.
[23] Southampton Electrochemistry Group, Instrumental Methods in Electrochemistry, Ellis Horwood Limited, Chichester, 1985.
[24] R.O. Lezna, S. Juanto, J.H. Zagal, J. Electroanal. Chem. 389 (1995) 197–200.
[25] G.L. Hugh, Y. Wang, C. Schöneich, P.-Y. Jiang, R.W. Fesenden, Radiat. Phys. Chem. 54 (1999) 559–566.
[26] G.V. Buxton, C.L. Greenstock, W.P. Hellman, A.B. Ross, W. Tsang, J. Phys. Chem. Ref. Data 17 (1988) 513–886.
[27] N. Getoff, A. Ritter, F. Schworer, Radiat. Phys. Chem. 41 (1993) 797–801.
[28] L.M. Dorfman, in: R.F. Gould (Ed.), The Solvated Electron in Organic Liquids, Adv. Chem Series, Am. Chem. Soc., Washington, DC, 1965.
[29] M. Simic, P. Neta, E. Hayon, J. Phys. Chem. 73 (1969) 3794–3800.
[30] M.R. Feliz, G. Ferraudi, Inorg. Chem. 37 (1998) 2806–2810.
[31] P. Hiort, B. Lincoln, B. Nordén, J. Am. Chem. Soc. 115 (1993) 3448–3454.
[32] J.E. Dickeson, L.A. Summers, Aust. J. Chem. 23 (1970) 1023–1028.
[33] W.D. Bates, Ph.D. dissertation, University of North Carolina at Chapel Hill, Chapel Hill, NC, 1995.
[34] S. Hotchandani, A.C. Testa, J. Photochem. Photobiol. A Chem. 55 (1991) 323–328.
[35] J.R. Huber, M. Mahaney, J.V. Morris, Chem. Phys. Lett. 16 (1976) 329–335.
[36] Y.H. Li, E.C. Lim, Chem. Phys. Lett. 9 (1971) 279–283.
[37] Y.H. Li, E.C. Lim, J. Chem. Phys. 47 (1971) 3270–3275.
[38] J.M. Kelly, C.M. Creely, S. Hudson, W.J. Blant, B. Elias, A. Kirsch-De Mesmaeker, P. Matonsek, M. Towrie, A.W. Parker, Central Laser Facility, Annual Report, 2001/2002, pp. 111–114.
[39] G.A. Davis, J.D. Gresser, P.A. Carapellucci, J. Am. Chem. Soc. 93 (1971) 2179–2182.
[40] G.N.R. Tripathi, Y. Su, J. Bentley, J. Am. Chem. Soc. 117 (1995) 5540–5549.
[41] G.N.R. Tripathi, Y. Su, J. Bentley, R.W. Fessenden, P.-Y. Jiang, J. Am. Chem. Soc. 118 (1996) 2245–2256.
[42] J. Fees, W. Kaim, M. Moscherosch, W. Matheis, J. Klima, M. Krejcik, S. Zalis, Inorg. Chem. 32 (1993) 166–174.
[43] A. Lewanowicz, J. Lipinski, J. Mol. Struct. 450 (1998) 163–169.
[44] G. Ferraudi, in: A.B.P. Lever, C.C. Leznoff (Eds.), Phthalocyanines. Properties and Applications, vol. 1, VCH, NY, 1996 (Chapter 4).